Published in final edited form as:
Anat Rec (Hoboken). 2011 October ; 294(10): 1624–1634. doi:10.1002/ar.21380.

Temporal and regional alterations in NMDA receptor expression in *Mecp2*-null mice

Mary E. Blue[1,2,3], **Walter E. Kaufmann**[1,2,4,5,6,7], **Joseph Bressler**[1,8], **Charlotte Eyring**[1], **Cliona O'Driscoll**[1], **SakkuBai Naidu**[1,2,5], and **Michael V. Johnston**[1,2,5]

[1]Hugo W. Moser Research Institute at Kennedy Krieger, Inc

[2]Department of Neurology, Johns Hopkins University School of Medicine

[3]Department of Neuroscience, Johns Hopkins University School of Medicine

[4]Department of Pathology, Johns Hopkins University School of Medicine

[5]Department of Pediatrics, Johns Hopkins University School of Medicine

[6]Department of Psychiatry and Behavioral Sciences, Johns Hopkins University School of Medicine

[7]Department of Radiology and Radiological Science, Johns Hopkins University School of Medicine

[8]Department of Environmental Health Sciences at the Bloomberg School of Public Health at Johns Hopkins University

Abstract

Our previous postmortem study of girls with Rett Syndrome (RTT), a development disorder caused by *MECP2* mutations, found increases in the density of NMDA receptors in the prefrontal cortex of 2–8 year-old girls, while girls older than 10 years had reductions in NMDA receptors compared to age matched controls (Blue et al., 1999b). Using [^{3}H]-CGP to label NMDA type glutamate receptors in 2 and 7 week old wildtype (WT), *Mecp2*-null and *Mecp2*-heterozygous (HET) mice (Bird model), we found that frontal areas of the brain also exhibited a bimodal pattern in NMDA expression, with increased densities of NMDA receptors in *Mecp2*-null mice at 2 weeks of age, but decreased densities at 7 weeks of age. Visual cortex showed a similar pattern, while other cortical regions only exhibited changes in NMDA receptor densities at 2 weeks (retrosplenial granular) or 7 weeks (somatosensory). In thalamus of null mice, NMDA receptors were increased at 2 and 7 weeks. No significant differences in density were found between HET and WT mice at both ages. Western blots for NMDAR1 expression in frontal brain showed higher levels of expression in *Mecp2*-null mice at two weeks of age, but not at 1 or 7 weeks of age. Our mouse data support the notion that deficient MeCP2 function is the primary cause of the NMDA receptor changes we observed in RTT. Furthermore, the findings of regional and temporal differences in NMDA expression illustrate the importance of age and brain region in evaluating different genotypes of mice.

Corresponding author to whom all correspondence should be sent: Mary E. Blue, PhD, Hugo W. Moser Research Institute at Kennedy Krieger, Inc., 707 North Broadway, Baltimore, MD 21205, Phone: 443 923-2693, FAX: 443 923-2695, blue@kennedykrieger.org.

Keywords

Rett syndrome; NMDA; Mouse models; Development

INTRODUCTION

Rett Syndrome (RTT) is a neurodevelopmental disorder that primarily affects girls. Phenotypic features include intellectual disability, motor dysfunction, seizures, and stereotyped movements (Rett, 1966; Hagberg et al., 1985; Neul et al., 2010). The large majority of RTT cases are caused by mutations in the X linked gene that encodes for methyl-CpG binding protein 2 (MeCP2) (Sirianni et al., 1998; Amir et al., 1999; Hoffbuhr et al., 2001). Mice with *Mecp2* mutations or that are deficient in Mecp2 show neuropathological and behavioral deficits similar to that reported for RTT (Chen et al., 2001; Guy et al., 2001; Shahbazian et al., 2002; Lawson-Yuen et al., 2007; Jentarra et al., 2010).

Neuropathological and neuroimaging changes in RTT point to an abnormality in maturation of synapses that preferentially affects certain regions and neuronal populations (Johnston et al., 2001). In RTT, deceleration of head circumference appears in the first few months of life at a time when the surge in proliferation of neuronal axo-dendritic connections is contributing to an exponential phase in brain growth (Naidu, 1997). A microarray analysis of postmortem brain from girls with RTT shows reductions in synaptic markers (Colantuoni et al., 2001), and the analysis of olfactory receptor neurons from biopsies from girls with RTT and *Mecp2*-null mice provides evidence for a block in the maturation of synapses (Cohen et al., 2003; Ronnett et al., 2003; Matarazzo et al., 2004; Palmer et al., 2008; Degano et al., 2009). Our previous studies find that the developmental expression of Mecp2 protein is most closely correlated with the timing of synapse formation (Johnston et al., 2003; Mullaney et al., 2004; Johnston et al., 2005; Kaufmann et al., 2005).

Neurophysiological studies also show abnormalities in synaptic circuitry in mouse models of RTT, including changes in LTP and LTD or connectivity (Asaka et al., 2006; Moretti et al., 2006; Dani and Nelson, 2009) and in EEG activity (D'Cruz et al., 2010). Dani et al. (Dani et al., 2005) reported that the balance between cortical excitation and inhibition in spontaneous activity of pyramidal neurons was shifted in favor of inhibition. On the other hand, Zhang et al. showed diminished basal inhibitory rhythmic activity in the CA3 circuit in *Mecp2*-Null mice, which rendered hippocampal circuitry prone to hyperexcitability (Zhang et al., 2008). Medrihan et al. (Medrihan et al., 2008) also found that GABAergic but not glycinergic synaptic neurotransmission was strongly suppressed in the *Mecp2*-null mouse (Bird model).

Other evidence supports the hypothesis that synaptic circuitry is hyperexcitable in young girls with RTT. Distinctive features of the RTT phenotype, such as hand stereotypies, breathing abnormalities, and high incidence of seizures, likely reflect enhanced excitatory activity in young girls with the disorder. In addition, CSF studies have shown elevations in glutamate levels (Hamberger et al., 1992; Lappalainen and Riikonen, 1996), and MR spectroscopy studies show an elevated glutamate/glutamine peak in young girls with RTT (Pan et al., 1999; Horska et al., 2009). Gene expression profiling studies of frontal cortex from girls with RTT show elevations in mRNAs for the NR1 NMDA receptor subunit, the

metabotropic mGluR1 receptor and the glial EAAT1 glutamate transporter (Colantuoni et al., 2001). In our 1999 postmortem study, we found that NMDA receptors were elevated in frontal cortex from girls younger than 8 years with RTT compared to age matched controls, but in girls with RTT 10 years and older, NMDA receptor density was reduced compared to controls (Blue et al., 1999b). This bimodal pattern resembled the clinical pattern of regression associated with encephalopathy and seizures followed by a plateau phase in most girls with RTT.

In the present study we further explore the hypothesis of disrupted excitatory synaptic function in RTT. Our goal was to determine whether Mecp2 deficiency in mice leads to a change in NMDA receptor expression that is similar to what we observed in our human studies. We used the same methodology applied to the human studies, receptor autoradiography, to examine NMDA receptor expression in the Bird model of Mecp2 deficiency. NMDA receptor expression was examined at two ages that corresponded roughly with the ages in humans that showed alterations in NMDA expression over development. We also used Western blots to measure the expression of the requisite NMDAR1 subunit to confirm our autoradiographic results.

MATERIALS AND METHODS

Animal Procedures

All of the procedures for animal use were reviewed and approved by the Animal Care and Use Committee at The Johns Hopkins University School of Medicine. Mecp2$^{tm1.1Bird}$ mice (Jackson Laboratory, Bar Harbor, Maine) on a C57BL/6 background (heterozygote backcrossed with C57BL/6 males for at least 9 generations) were used. Tail-clipping samples were obtained between P4 and P7 for genotyping, which was performed by PCR using a protocol provided by Jackson Laboratory. For autoradiography, all three genotypes of mice were evaluated at 2 weeks and 7 weeks of age (for 2 weeks, n=10–14 WT, n=3–5 HET and n=6–8 *Mecp2*-null; for 7 weeks, n=9–11 WT, 4–5 HET, and n=5–6 *Mecp2*-null). For Western blots, WT and *Mecp2*-null mice were studied (for 1 week, n=10 WT and n=10 *Mecp2*-null; for 2 weeks, n=6 WT and n=7 *Mecp2*-null; for 7 weeks, n=6 WT and n=5 *Mecp2*-null). Mice were anesthetized, decapitated and the brains were removed rapidly and frozen on dry ice. Brains were kept at −80°C until the brains were sectioned (autoradiography) or blocks of tissue were cut (Western blots).

Autoradiography

Sections were cut on a Microm cryostat at 20 μm thickness, thaw mounted on Super-frost plus slides and stored at −80°C prior to receptor labeling. NMDA receptor binding sites were labeled as described previously (Jaarsma et al., 1993; Blue et al., 1999a; Blue et al., 1999b) with 20 nM [^{3}H] CGP39653 ([^{3}H] CGP) in 50 mM Tris-HCl (pH, 8.0, 4°C); 30 U/ml glutamate dehydrogenase, 0.03% (v/v) hydrazine and 1.1 mM NAD+ were added to the incubation buffer to remove residual endogenous l-glutamate. Nonspecific binding was determined using a 100 μM DL-AP5 blank. Autoradiographically labeled sections were apposed to Amersham [^{3}H] tritium sensitive Hyperfilm for 6–12 months and developed photographically using D-19 and Rapid-fix (Kodak). Afterwards, the sections were stained

with cresyl violet (Nissl-stain) to identify specific regions of interest (ROI). The films were analyzed using a video based image analysis system (InterFocus Imaging Ltd., Cambridge, England) as described previously (Blue et al., 1997; Brennan et al., 1997; Blue et al., 1999a; Blue et al., 1999b). Using surface and interior landmarks, each brain was divided into different rostral-caudal levels. In every section that was analyzed, the ROI was outlined based on its location on the Nissl-stained section, and the density within each ROI was measured in each hemisphere. Figure 1 shows the five rostral-caudal levels where density measurements were made and each ROI measured at each level. At each rostro-caudal level, density values for each ROI were determined by averaging the values for the right and left sides of the brain; if 2 sections were present at each level, the values also were averaged. For regions spanning the different rostral-caudal levels, measurements were averaged, i.e., for insula, the density represents the average of the measurements at three rostro-caudal levels. Due to run-to-run variability, density values were expressed as percent of WT mice. Analyses of variance (ANOVA) and t-tests were performed using Prism Graph Pad to determine whether the density of NMDA receptors varied by genotype, region or by age. If significant variances were found among the different genotypes in ANOVA or t-test analyses, non-parametric tests were used.

A separate analysis was performed for individual regions within the hippocampus. The regions within the hippocampus studied are shown in Figure 2. The hippocampus analysis was performed at two levels, through the dorsal hippocampus and through the ventral hippocampus (Figure 1D and 1E). As above, the density values represent the average of measurements in the right and left hemisphere from one (dorsal hippocampus) or two (ventral hippocampus) sections, and as percent WT.

Western Blots

The protein expression of the NMDAR1 subunit of the NMDA receptor was measured in 1, 2 and 7 week old WT and *Mecp2*-null mice as described previously (Mullaney et al., 2004). For these studies, mice were anesthetized and euthanized and the brains quickly removed and frozen on powdered dry ice and then the tissue was stored in a −80°C freezer. We isolated a block from the prefrontal region of the brain for Western blotting by making a cut perpendicular to the surface of the brain that extended as far back as the olfactory bulb, but which did not include the olfactory bulb (2–5 mm). The tissue was suspended in cold RIPA (150 mM NaCl, 1.0% IGEPAL® CA-630, 0.5% sodium deoxycholate, 0.1% SDS, and 50 mM Tris, pH 8.0.) containing protease inhibitors (Calbiochem) and briefly sonicated. After determination of protein concentration, 30 μg of protein homogenate was resolved by sodium dodecylsulfate polyacrylamide gel electrophoresis on a 4–20% gradient gel (Invitrogen), followed by transfer onto nitrocellulose membranes, and incubation with primary antibodies to the NMDAR1 subunit of the NMDA receptor (#4204, Cell Signaling, 1:1000) and β-actin (#A5316, Sigma, 1:5000) (as described (Sun et al., 2001; Aber et al., 2003). This was followed by signal detection using specific infrared secondary antibodies (Jackson, 1:10000). Data was analyzed using the 2-color near infrared Odyssey system (LI-COR Biosciences, Lincoln, NE). We performed t-tests using Prism Graph Pad to determine whether the density of NMDA receptors varied between *Mecp2*-null and WT mice.

RESULTS

The results of our autoradiographic study show that [^{3}H] CGP binding to NMDA receptors varies by genotype, age and region. At 2 weeks of age, the densities of NMDA receptors in frontal areas of the cerebral cortex and striatum of *Mecp2*-null mice are greater than in WT mice, while at 7 weeks of age, densities of NMDA receptors are reduced in null mice (Figures 3–5; Table 1). This bimodal pattern of the NMDA receptor changes with age resembles that previously observed in our postmortem study of girls with RTT (Blue et al., 1999b). The region exhibiting the greatest magnitude of developmental changes in null mice was the insula. Figure 6 shows the mean densities for each rostro-caudal level of the insula measured. Compared to WT mice, NMDA receptor density is increased by 71% in the null mice at the prefrontal level of the insula, at 2 weeks, while it is reduced by 37% at 7 weeks. In contrast, at the mid-frontal level, the insula has less striking changes in NMDA expression among the different genotypes of mice, especially at 7 weeks (Figure 4).

The visual cortex exhibits a similar bimodal pattern, although the differences between WT and *Mecp2*-null mice do not quite reach significance at 2 weeks of age (Figure 5D). In somatosensory cortex, NMDA receptor density in *Mecp2*-null mice at 2 weeks of age is not different from the WT, but at 7 weeks of age, NMDA receptor density is reduced in *Mecp2*-null mice compared to WT mice (Figure 5E). In retrosplenial granular cortex (RS), another pattern emerges such that at 2 weeks of age, NMDA receptor density is increased in *Mecp2*-null mice, but by 7 weeks of age is similar to that for WT mice (Figure 5F). In thalamus, the density of NMDA receptors remains higher in *Mecp2*-null mice than in WT mice at both 2 and 7 weeks (Figure 5G). NMDA receptor density in the hippocampus of *Mecp2*-null mice is not significantly different from the WT at either age (Figure 5H). However, an analysis of specific regions and layers in the hippocampus does show significant differences in density between WT and Mecp2-null mice (Tables 2 and 3). At 2 weeks of age, the density of NMDA receptors was increased in the stratum oriens at both levels of the hippocampus and in the pyramidal cell layer of CA3, the dentate gyrus, granular cell layer of the dentate, and subiculum at the level of the ventral hippocampus in *Mecp2*-null mice compared to WT mice. At 7 weeks of age, NMDA receptor density remained elevated in the stratum oriens and radiatum of CA3 at the level of the ventral hippocampus in the null mice relative to the WT.

The results of Western blot analyses of NMDAR1 expression from blocks of tissue from the prefrontal regions of the brain from *Mecp2*-null and WT mice at 1, 2 and 7 weeks of age show significant age related differences in NR1 expression (Figure 7). At 1 and 2 weeks of age, mean NR1 expression values are higher in *Mecp2*-null than in WT mice (Figure 7A). While at 1 week this difference is not significant due to variability in both samples, at 2 weeks of age, the difference is significant ($p<0.05$; Figure 7B). By 7 weeks of age, no significant genotype differences in NR1 expression are observed.

DISCUSSION

The results of the current study indicate that NMDA receptor expression is altered in mice that are lacking Mecp2 expression. The modifications in NMDA expression are age and

region dependent. We find a bimodal pattern in NMDA expression in prefrontal and frontal regions (frontal motor areas, insular cortex and striatum) of the brain, with increased expression of NMDA receptors in *Mecp2*-null mice at 2 weeks of age, but decreased expression at 7 weeks of age. The visual cortex shows a similar trend. Western blot analyses show a pattern of NMDAR1 expression in prefrontal areas of the brain that is consistent with our autoradiographic results from mice that are 2 weeks of age. Here too, NMDAR1 expression is higher in *Mecp2*-null mice than in the WT at 2 weeks of age, while equivalent levels are observed in both genotypes at 7 weeks of age. The high correlation between our receptor autoradiography and Western blot results indicates that the changes in NMDA density are not due to reductions in postsynaptic area, but rather that the loss of Mecp2 is responsible for the changes in NMDA receptor expression.

Other cortical regions, such as retrosplenial granular cortex showed increased expression of NMDA receptors in *Mecp2*-null mice at 2 weeks of age, but no difference at 7 weeks of age. A third pattern was found in the somatosensory cortex that had equivalent levels of NMDA expression in *Mecp2*-null and WT mice at 2 weeks of age, but by 7 weeks of age, NMDA receptor density in the null mice was significantly lower than in the WT mice. Finally, the thalamus and specific layers and regions of the hippocampus in null mice show increased expression of NMDA receptors at both 2 and 7 weeks of age.

The density of NMDA receptors in HET mice showed more variability than in WT or *Mecp2*-null mice. As a result, no significant differences in density were found between HET and WT mice at both ages. These observations differ from our autoradiography studies in autopsied brain tissue of girls with RTT where we found that in younger girls there is a significant increase (38% $p=0.02$) in NMDA receptors in the frontal lobes, while in older subjects aged >10 years NMDA receptor density is reduced by 37% when compared to age matched controls. The differences between the results of the studies in HET mice and RTT patients, essentially heterozygous for *MECP2* mutations, could be related to differences in X-inactivation status. Others have shown that X-inactivation is skewed in HET mice, with significantly more cells expressing the wild-type allele (Braunschweig et al., 2004; Young and Zoghbi, 2004).

Understanding the alterations in NMDA receptor expression in the context of the observed changes in glutamate levels and synaptic transmission may provide some clues to the effects of decreased MeCP2 function on brain development. Glutamate levels as measured by spectroscopy are either unchanged or decreased in the brains of *Mecp2*-null mice, depending on the age of the animal (Saywell et al., 2006; Viola et al., 2007; Ward et al., 2008). One study showed reductions in glutamate levels in 2–3 week old and 7 week old null mice (Ward et al., 2008), while glutamate levels in 4–5 week old were not different (Ward et al., 2008). Two other studies by another group did not find differences in glutamate levels of 5–8 week old null mice compared to the WT (Saywell et al., 2006; Viola et al., 2007). At 2 weeks of age, we found that NMDA receptor expression was generally increased in the null mice. These elevations in NMDA receptor density could represent an attempt to compensate for the decreased levels of glutamate and thus maintain the homeostatic state. For example, in the presymptomatic phase, which is up to 5 weeks of age, short and long term potentiation (STP, LTP) and long term depression (LTD) remain intact in null mice (Asaka et al., 2006).

However, the increased density of NMDA receptors at this early stage of postnatal development, could account for the increased susceptibility to excitotoxicity induced by hypoxia or exposure to glutamate receptor agonists that also is observed in cultured neurons of null mice (Russell et al., 2007) and in null mice (Fischer et al., 2009).

Once the null mice become symptomatic, beginning at 5–6 weeks of age and lasting until death, a different pattern emerges. We observe significant decreases in NMDA expression in the 7 week old mice, while other studies show decreases in Glu levels (Ward et al., 2008), in STP and LTP (Asaka et al., 2006), in glutamate receptor mediated currents (Zhang et al., 2008), reduced expression of the NR1, and NR2A subunits, and decreases in the NR2A/NRB ratio (Maliszewska-Cyna et al., 2010). These findings suggest that the homeostatic state has been disrupted. As a result, synaptic function is altered (D'Cruz et al., 2010) and connectivity is reduced (Dani and Nelson, 2009).

We examined NMDA expression in the insula and retrosplenial granular cortex (RSG), as they are two regions in RTT that underlie the central parietal and frontal regions, where abnormal EEGs and seizures arise in girls with RTT. Our results showed dramatic age related changes in NMDA receptors in the insula of *Mecp2* null mice. The insula is involved in the pathogenesis of several aspects of the RTT phenotype, including seizures, autonomic dysfunction and speech impairment (Ackermann and Riecker, 2010; Nagai et al., 2010). The retrosplenial granular cortex (RSG) was another area showing significant increases in NMDA receptor expression in the 2-week-old *Mecp2*-null mice. This region is connected with limbic structures that are implicated in epilepsy, such as the hippocampus and the parahippocampal gyrus (Cardoso et al., 2008). Recent studies have shown that experimentally induced seizures in rats and mice adversely affect the RSG (Ampuero et al., 2007; Cardoso et al., 2008; Kukko-Lukjanov et al., 2010). The striking increase in NMDA receptor expression in both the RSG and the insula, at two weeks of age, may make these regions particularly hyperexcitable, as has been reported in other brain regions of *Mecp2*-null mice (Zhang et al., 2008; D'Cruz et al., 2010).

The pattern of NMDA receptor changes in MeCP2 deficient mice resembles the bimodal age-dependent pattern we reported in patients with RTT (Blue et al., 1999b). Although we did not examine the insular cortex in humans, elevated density at earlier ages and decreased density at more mature stages seem to be a signature for frontal NMDA receptors in the MeCP2-deficient brain. While a compensatory mechanism can be invoked for young *Mecp2*-null mice, in humans the relationship between glutamate levels and NMDA receptor seems to be more complex. We and others have shown that glutamate levels are increased in RTT patients; in our recent MR spectroscopy study these differences were present mainly in subjects younger than 10 years (Horska et al., 2009), the same period characterized by elevated NMDA receptors (Blue et al., 1999b). The elevated glutamate levels along with increased NMDA expression in RTT suggests an inability of the brain to compensate for the changes in glutamate levels. This is similar to the cholinergic findings in RTT, where decreases in choline acetyltransferase and in [^{3}H]-vesamicol binding to a terminal vesicular acetylcholine transporter are found in the putamen and thalamus, whereas normally, an inverse relationship exists (Wenk and Mobley, 1996). Several authors have noted the phenotypical differences between Mecp2-deficient mice and patients with RTT; even a

complete absence of Mecp2 expression in mice does not lead to the severe neurologic phenotype observed in humans (Chen et al., 2001; Guy et al., 2001). One plausible explanation is the greater synaptic complexity of humans, which leads to a greater dependence on synaptic regulators such as MeCP2 (LaSalle, 2004; Kaufmann et al., 2005). Similar phenotypical severity discrepancies between FMRP-deficient mice and patients with fragile X syndrome seem to support this hypothesis (Hagerman et al., 2009).

Unlike other brain regions, NMDA receptor binding was increased in the thalamus and in various layers of CA3 and the dentate gyrus of the hippocampus (especially the ventral hippocampus) in *Mecp2*-null mice at both 2 and 7 weeks of age. This enduring increase in NMDA receptors indicates that the thalamus and hippocampus may be in a persistent hyperexcitable state in Mecp2 deficiency. In the thalamus, Zhang et al (2010) showed that mIPSCs were decreased and that the number of GABA transporters was decreased in the ventrobasal (VB) thalamus (P6, P14–16 and P21) in *Mecp2*-null mice. The VB thalamus projects to somatosensory cortex and insula. Our findings that NMDA receptor expression is increased in VB along with the Zhang data may indicate that the thalamus is overdriving the cortex. Alternatively, the changes in NMDA receptor may represent a compensatory response to decreases in choline acetyltransferase (Wenk and Mobley, 1996). In hippocampus, the increases in NMDA expression at 2 weeks of age may explain the preserved LTD and LTP in presymptomatic *Mecp2*-null mice (Asaka et al., 2006), while the increases in NMDA receptor density in the stratum oriens and stratum radiatum of 7 week-old *Mecp2*-null mice may account for the hyperexcitable state of this circuit in symptomatic null mice (Zhang et al., 2008).

Taken together, the results of this study indicate the importance of considering age of development and region when determining changes in neurotransmitter expression in a mouse model for RTT and when designing therapeutic trials. The increased expression of NMDA receptors in young *Mecp2* null mice and girls with RTT indicate that NMDA receptor antagonists may be effective in alleviating some of the symptoms. In fact, one of the authors (S.N.) has an ongoing study administering dextromethorphan (DM), a partial NMDA antagonist, to girls with RTT between the ages of 2–10 years. Preliminary results show that DM is safe and tolerated well; as the study is ongoing we cannot report on the efficacy of the treatment. After the age of 10, however, it may be more efficacious consider the use of NMDA or AMPA agonists.

Acknowledgments

We thank Ms. Jennifer Berrong, Ms. Karen Smith-Connor and Ms. Kristen Talbot for technical assistance. This work was supported by NICHD grants HD 24448 and HD24061.

LITERATURE CITED

Aber KM, Nori P, MacDonald SM, Bibat G, Jarrar MH, Kaufmann WE. Methyl-CpG-binding protein 2 is localized in the postsynaptic compartment: an immunochemical study of subcellular fractions. Neuroscience. 2003; 116:77–80. [PubMed: 12535940]

Ackermann H, Riecker A. The contribution(s) of the insula to speech production: a review of the clinical and functional imaging literature. Brain Struct Funct. 2010; 214:419–433. [PubMed: 20512374]

Amir RE, Van den Veyver IB, Wan M, Tran CQ, Francke U, Zoghbi HY. Rett syndrome is caused by mutations in X-linked MECP2, encoding methyl-CpG-binding protein 2. Nat Genet. 1999; 23:185–188. [PubMed: 10508514]

Ampuero E, Dagnino-Subiabre A, Sandoval R, Zepeda-Carreno R, Sandoval S, Viedma A, Aboitiz F, Orrego F, Wyneken U. Status epilepticus induces region-specific changes in dendritic spines, dendritic length and TrkB protein content of rat brain cortex. Brain Res. 2007; 1150:225–238. [PubMed: 17397806]

Asaka Y, Jugloff DG, Zhang L, Eubanks JH, Fitzsimonds RM. Hippocampal synaptic plasticity is impaired in the Mecp2-null mouse model of Rett syndrome. Neurobiol Dis. 2006; 21:217–227. [PubMed: 16087343]

Blue ME, Martin LJ, Brennan EM, Johnston MV. Ontogeny of non-NMDA glutamate receptors in rat barrel field cortex: I. Metabotropic receptors. J Comp Neurol. 1997; 386:16–28. [PubMed: 9303522]

Blue ME, Naidu S, Johnston MV. Altered development of glutamate and GABA receptors in the basal ganglia of girls with Rett syndrome. ExpNeurol. 1999a; 156:345–352.

Blue ME, Naidu S, Johnston MV. Development of amino acid receptors in frontal cortex from girls with Rett syndrome. Ann Neurol. 1999b; 45:541–545. [PubMed: 10211484]

Braunschweig D, Simcox T, Samaco RC, LaSalle JM. X-Chromosome inactivation ratios affect wild-type MeCP2 expression within mosaic Rett syndrome and Mecp2−/+ mouse brain. Hum Mol Genet. 2004; 13:1275–1286. [PubMed: 15115765]

Brennan EM, Martin LJ, Johnston MV, Blue ME. Ontogeny of non-NMDA glutamate receptors in rat barrel field cortex: II. AMPA and kainate receptors. J Comp Neurol. 1997; 386:29–45. [PubMed: 9303523]

Cardoso A, Madeira MD, Paula-Barbosa MM, Lukoyanov NV. Retrosplenial granular b cortex in normal and epileptic rats: a stereological study. Brain Res. 2008; 1218:206–214. [PubMed: 18533134]

Chen RZ, Akbarian S, Tudor M, Jaenisch R. Deficiency of methyl-CpG binding protein-2 in CNS neurons results in a Rett-like phenotype in mice. Nat Genet. 2001; 27:327–331. [PubMed: 11242118]

Cohen DR, Matarazzo V, Palmer AM, Tu Y, Jeon OH, Pevsner J, Ronnett GV. Expression of MeCP2 in olfactory receptor neurons is developmentally regulated and occurs before synaptogenesis. Mol Cell Neurosci. 2003; 22:417–429. [PubMed: 12727440]

Colantuoni C, Jeon OH, Hyder K, Chenchik A, Khimani AH, Narayanan V, Hoffman EP, Kaufmann WE, Naidu S, Pevsner J. Gene expression profiling in postmortem Rett Syndrome brain: differential gene expression and patient classification. Neurobiol Dis. 2001; 8:847–865. [PubMed: 11592853]

D'Cruz JA, Wu C, Zahid T, El-Hayek Y, Zhang L, Eubanks JH. Alterations of cortical and hippocampal EEG activity in MeCP2-deficient mice. Neurobiol Dis. 2010; 38:8–16. [PubMed: 20045053]

Dani VS, Chang Q, Maffei A, Turrigiano GG, Jaenisch R, Nelson SB. Reduced cortical activity due to a shift in the balance between excitation and inhibition in a mouse model of Rett syndrome. Proc Natl Acad Sci U S A. 2005; 102:12560–12565. [PubMed: 16116096]

Dani VS, Nelson SB. Intact long-term potentiation but reduced connectivity between neocortical layer 5 pyramidal neurons in a mouse model of Rett syndrome. J Neurosci. 2009; 29:11263–11270. [PubMed: 19741133]

Degano AL, Pasterkamp RJ, Ronnett GV. MeCP2 deficiency disrupts axonal guidance, fasciculation, and targeting by altering Semaphorin 3F function. Mol Cell Neurosci. 2009; 42:243–254. [PubMed: 19628041]

Fischer M, Reuter J, Gerich FJ, Hildebrandt B, Hagele S, Katschinski D, Muller M. Enhanced hypoxia susceptibility in hippocampal slices from a mouse model of rett syndrome. J Neurophysiol. 2009; 101:1016–1032. [PubMed: 19073793]

Guy J, Hendrich B, Holmes M, Martin JE, Bird A. A mouse *Mecp2*-null mutation causes neurological symptoms that mimic Rett syndrome. Nat Genet. 2001; 27:322–326. [PubMed: 11242117]

Hagberg B, Goutieres F, Hanefeld F, Rett A, Wilson J. Rett syndrome: criteria for inclusion and exclusion. Brain Dev. 1985; 7:372–373. [PubMed: 4061772]

Hagerman RJ, Berry-Kravis E, Kaufmann WE, Ono MY, Tartaglia N, Lachiewicz A, Kronk R, Delahunty C, Hessl D, Visootsak J, Picker J, Gane L, Tranfaglia M. Advances in the treatment of fragile X syndrome. Pediatrics. 2009; 123:378–390. [PubMed: 19117905]

Hamberger A, Gillberg C, Palm A, Hagberg B. Elevated CSF glutamate in Rett syndrome. Neuropediatrics. 1992; 23:212–213. [PubMed: 1357572]

Hoffbuhr K, Devaney JM, LaFleur B, Sirianni N, Scacheri C, Giron J, Schuette J, Innis J, Marino M, Philippart M, Narayanan V, Umansky R, Kronn D, Hoffman EP, Naidu S. MeCP2 mutations in children with and without the phenotype of Rett syndrome. Neurology. 2001; 56:1486–1495. [PubMed: 11402105]

Horska A, Farage L, Bibat G, Nagae LM, Kaufmann WE, Barker PB, Naidu S. Brain metabolism in Rett syndrome: age, clinical, and genotype correlations. Ann Neurol. 2009; 65:90–97. [PubMed: 19194883]

Jaarsma D, Sebens JB, Korf J. Glutamate dehydrogenase improves binding of [3H]CGP39653 to NMDA receptors in the autoradiographic assay. J Neurosci Methods. 1993; 46:133–138. [PubMed: 7682638]

Jentarra GM, Olfers SL, Rice SG, Srivastava N, Homanics GE, Blue M, Naidu S, Narayanan V. Abnormalities of cell packing density and dendritic complexity in the MeCP2 A140V mouse model of Rett syndrome/X-linked mental retardation. BMC Neurosci. 2010; 11:19. [PubMed: 20163734]

Johnston MV, Blue ME, Naidu S. Rett syndrome and neuronal development. J Child Neurol. 2005; 20:759–763. [PubMed: 16225832]

Johnston MV, Jeon OH, Pevsner J, Blue ME, Naidu S. Neurobiology of Rett syndrome: a genetic disorder of synapse development. Brain Dev. 2001; 23(Suppl 1):S206–213. [PubMed: 11738874]

Johnston MV, Mullaney B, Blue ME. Neurobiology of Rett syndrome. J Child Neurol. 2003; 18:688–692. [PubMed: 14649550]

Kaufmann WE, Johnston MV, Blue ME. MeCP2 expression and function during brain development: implications for Rett syndrome's pathogenesis and clinical evolution. Brain Dev. 2005; 27(Suppl 1):S77–S87. [PubMed: 16182491]

Kukko-Lukjanov TK, Lintunen M, Jalava N, Lauren HB, Lopez-Picon FR, Michelsen KA, Panula P, Holopainen IE. Involvement of histamine 1 receptor in seizure susceptibility and neuroprotection in immature mice. Epilepsy Res. 2010; 90:8–15. [PubMed: 20359868]

Lappalainen R, Riikonen RS. High levels of cerebrospinal fluid glutamate in Rett syndrome. Pediatr Neurol. 1996; 15:213–216. [PubMed: 8916158]

LaSalle JM. Paradoxical role of methyl-CpG-binding protein 2 in Rett syndrome. Curr Top Dev Biol. 2004; 59:61–86. [PubMed: 14975247]

Lawson-Yuen A, Liu D, Han L, Jiang ZI, Tsai GE, Basu AC, Picker J, Feng J, Coyle JT. Ube3a mRNA and protein expression are not decreased in Mecp2R168X mutant mice. Brain Res. 2007; 1180:1–6. [PubMed: 17936729]

Maliszewska-Cyna E, Bawa D, Eubanks JH. Diminished prevalence but preserved synaptic distribution of N-methyl-d-aspartate receptor subunits in the methyl CpG binding protein 2-null mouse brain. Neuroscience. 2010

Matarazzo V, Cohen D, Palmer AM, Simpson PJ, Khokhar B, Pan SJ, Ronnett GV. The transcriptional repressor Mecp2 regulates terminal neuronal differentiation. Mol Cell Neurosci. 2004; 27:44–58. [PubMed: 15345242]

Medrihan L, Tantalaki E, Aramuni G, Sargsyan V, Dudanova I, Missler M, Zhang W. Early defects of GABAergic synapses in the brain stem of a MeCP2 mouse model of Rett syndrome. J Neurophysiol. 2008; 99:112–121. [PubMed: 18032561]

Moretti P, Levenson JM, Battaglia F, Atkinson R, Teague R, Antalffy B, Armstrong D, Arancio O, Sweatt JD, Zoghbi HY. Learning and memory and synaptic plasticity are impaired in a mouse model of Rett syndrome. J Neurosci. 2006; 26:319–327. [PubMed: 16399702]

Mullaney BC, Johnston MV, Blue ME. Developmental expression of methyl-CpG binding protein 2 is dynamically regulated in the rodent brain. Neuroscience. 2004; 123:939–949. [PubMed: 14751287]

Nagai M, Hoshide S, Kario K. The insular cortex and cardiovascular system: a new insight into the brain-heart axis. J Am Soc Hypertens. 2010; 4:174–182. [PubMed: 20655502]

Naidu S. Rett syndrome: a disorder affecting early brain growth. Ann Neurol. 1997; 42:3–10. [PubMed: 9225679]

Neul J, Kaufmann W, Glaze D, Christodoulou J, Clarke A, Bahi-Buisson N, Leonard H, Bailey M, Schanen N, Kerr A, Renieri A, Huppke P, Percy A. Consortium ftR. Rett syndrome: Revised diagnostic criteria and nomenclature. Ann Neurol. 2010 in press.

Palmer A, Qayumi J, Ronnett G. MeCP2 mutation causes distinguishable phases of acute and chronic defects in synaptogenesis and maintenance, respectively. Mol Cell Neurosci. 2008; 37:794–807. [PubMed: 18295506]

Pan JW, Lane JB, Hetherington H, Percy AK. Rett syndrome: 1H spectroscopic imaging at 4.1 Tesla. J Child Neurol. 1999; 14:524–528. [PubMed: 10456763]

Rett A. On a unusual brain atrophy syndrome in hyperammonemia in childhood. Wien Med Wochenschr. 1966; 116:723–726. [PubMed: 5300597]

Ronnett GV, Leopold D, Cai X, Hoffbuhr KC, Moses L, Hoffman EP, Naidu S. Olfactory biopsies demonstrate a defect in neuronal development in Rett's syndrome. Ann Neurol. 2003; 54:206–218. [PubMed: 12891673]

Russell JC, Blue ME, Johnston MV, Naidu S, Hossain MA. Enhanced cell death in MeCP2 null cerebellar granule neurons exposed to excitotoxicity and hypoxia. Neuroscience. 2007; 150:563–574. [PubMed: 17997046]

Saywell V, Viola A, Confort-Gouny S, Le Fur Y, Villard L, Cozzone PJ. Brain magnetic resonance study of Mecp2 deletion effects on anatomy and metabolism. Biochem Biophys Res Commun. 2006; 340:776–783. [PubMed: 16380085]

Shahbazian M, Young J, Yuva-Paylor L, Spencer C, Antalffy B, Noebels J, Armstrong D, Paylor R, Zoghbi H. Mice with truncated MeCP2 recapitulate many Rett syndrome features and display hyperacetylation of histone H3. Neuron. 2002; 35:243–254. [PubMed: 12160743]

Sirianni N, Naidu S, Pereira J, Pillotto RF, Hoffman EP. Rett syndrome: confirmation of X-linked dominant inheritance, and localization of the gene to Xq28. Am J Hum Genet. 1998; 63:1552–1558. [PubMed: 9792883]

Sun HT, Cohen S, Kaufmann WE. Annexin-1 is abnormally expressed in fragile X syndrome: two-dimensional electrophoresis study in lymphocytes. Am J Med Genet. 2001; 103:81–90. [PubMed: 11562939]

Viola A, Saywell V, Villard L, Cozzone PJ, Lutz NW. Metabolic fingerprints of altered brain growth, osmoregulation and neurotransmission in a Rett syndrome model. PLoS One. 2007; 2:e157. [PubMed: 17237885]

Ward BC, Agarwal S, Wang K, Berger-Sweeney J, Kolodny NH. Longitudinal brain MRI study in a mouse model of Rett Syndrome and the effects of choline. Neurobiol Dis. 2008; 31:110–119. [PubMed: 18571096]

Wenk GL, Mobley SL. Choline acetyltransferase activity and vesamicol binding in Rett syndrome and in rats with nucleus basalis lesions. Neuroscience. 1996; 73:79–84. [PubMed: 8783231]

Young JI, Zoghbi HY. X-chromosome inactivation patterns are unbalanced and affect the phenotypic outcome in a mouse model of rett syndrome. Am J Hum Genet. 2004; 74:511–520. [PubMed: 14973779]

Zhang L, He J, Jugloff DG, Eubanks JH. The MeCP2-null mouse hippocampus displays altered basal inhibitory rhythms and is prone to hyperexcitability. Hippocampus. 2008; 18:294–309. [PubMed: 18058824]

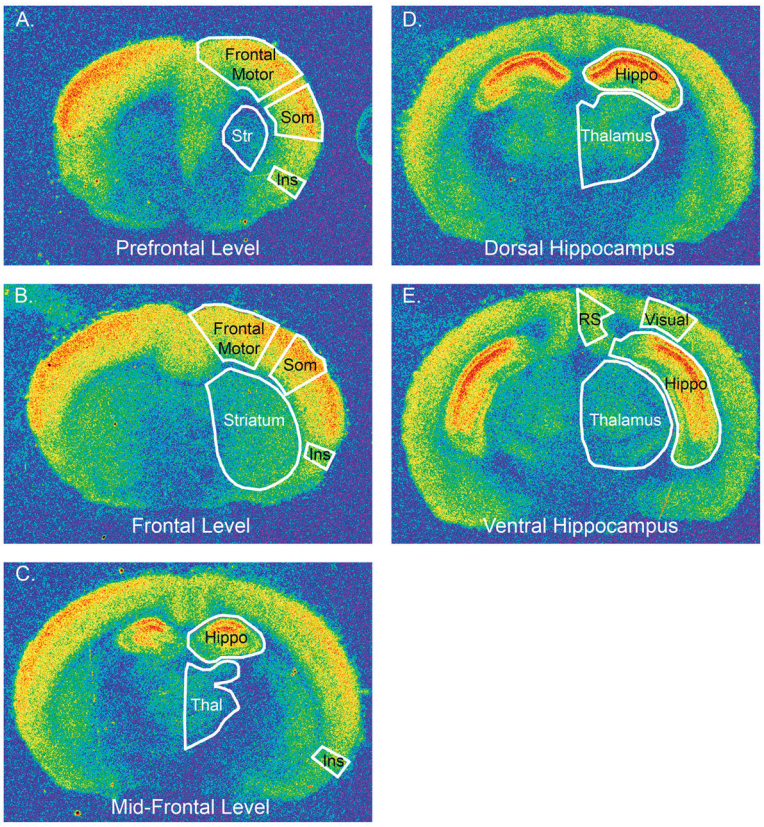

Figure 1.

Pseudocolor images of [^{3}H] CGP binding to NMDA receptors in sections from 2 week-old WT mice illustrate the different rostro-caudal levels where density measurements were made. At each level, the regions where densities were measured, are outlined in white and labeled. At prefrontal (A.) and frontal (B.) levels, the regions include frontal motor cortex, somatosensory cortex (Som), the insula (Ins) and the striatum (Str). At mid-frontal (C.) and dorsal hippocampus (D.) levels, NMDA densities were measured in the thalamus (Thal) and hippocampus (Hippo). NMDA receptor densities in the retrosplenial granular (RS) cortex, hippocampus and thalamus were measured at the level of the ventral hippocampus (E.).

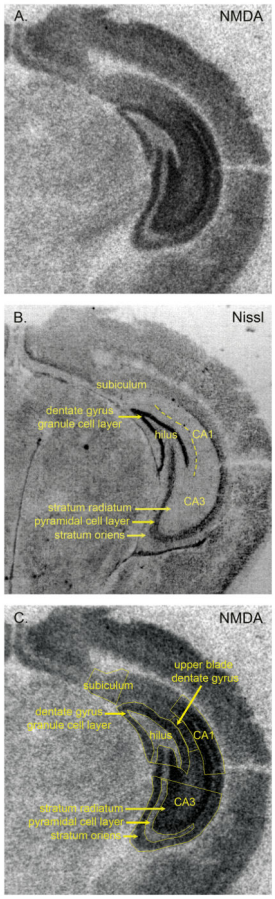

Figure 2.

Images of [^{3}H] CGP binding to NMDA receptors (A. and C.) and the corresponding Nissl stained section (B.) that illustrates the different regions and layers of the hippocampal formation that were measured. This section is from a 2 week-old WT mouse and is at the level of the ventral hippocampus.

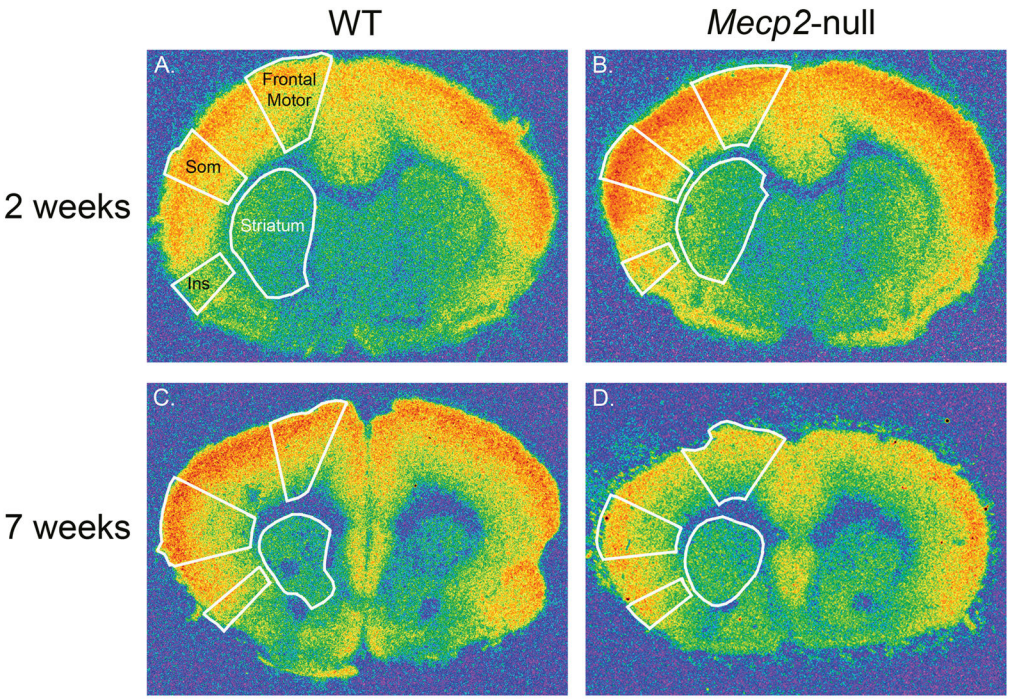

Figure 3.

Pseudocolor images of [^{3}H] CGP binding to NMDA receptors in sections through the frontal (A. and B.) and prefrontal levels (C. and D.) of the brain from WT (A. and C.) and *Mecp2*-null mice (B. and D.) at 2 and 7 weeks of age. The regions where densities were measured, are outlined in white in each section. These regions include frontal motor cortex, somatosensory cortex (Som), the insula (Ins) and the striatum (Str), and are labeled in A.

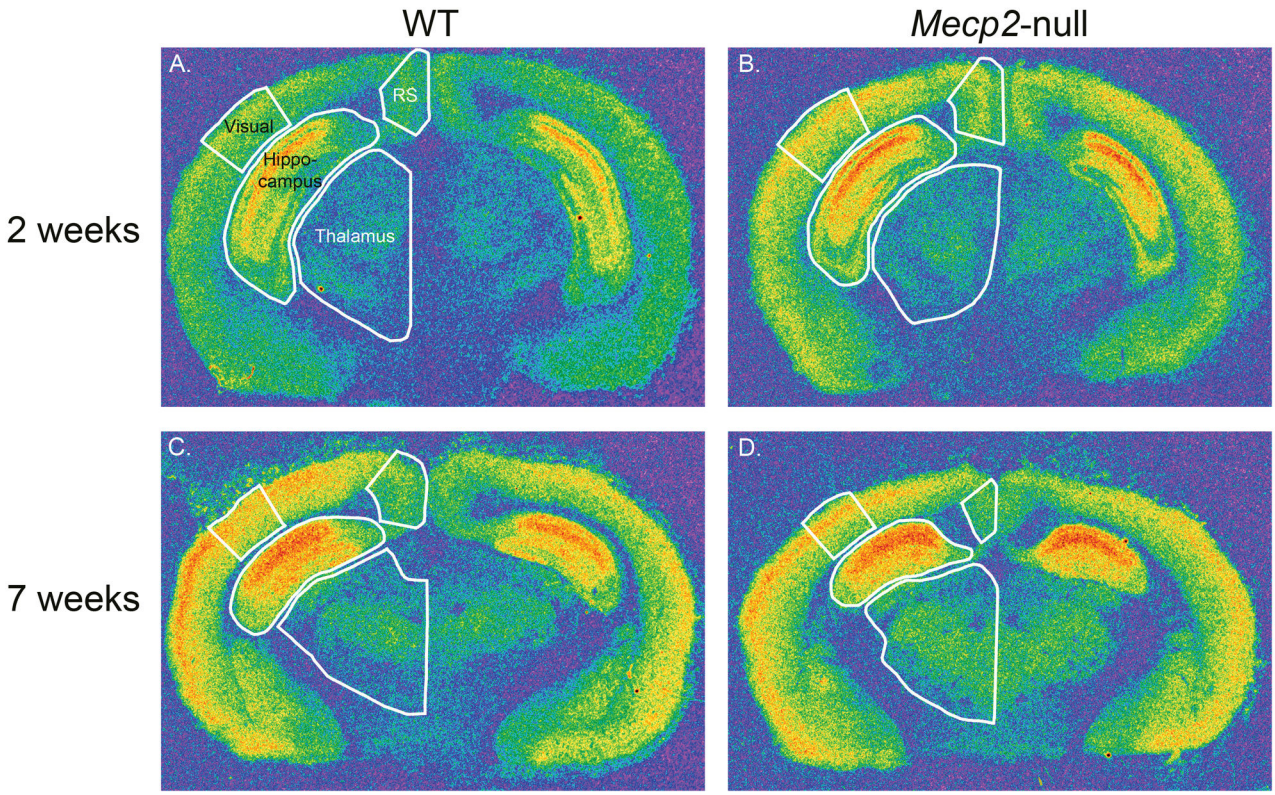

Figure 4.

Pseudocolor images of [^{3}H] CGP binding to NMDA receptors in sections through the dorsal hippocampus level of the brain from WT (A. and C.) and *Mecp2*-null mice (B. and D.) at 2 and 7 weeks of age. The regions where densities were measured are outlined in white in each section. These regions include visual cortex, retrosplenial granular (RS) cortex, hippocampus and thalamus, and are labeled in A.

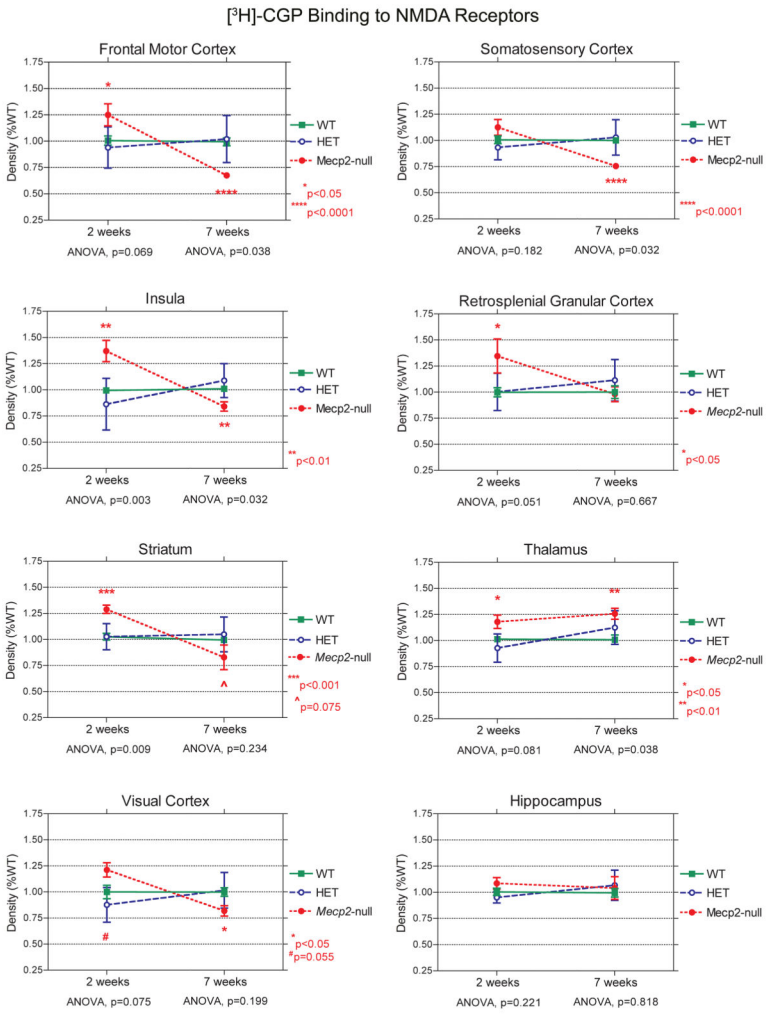

Figure 5.

Line graphs comparing the density of NMDA receptors (percent WT; mean ± s.e.m.) between WT and *Mecp2*-null mice at 2 and 7 weeks of age in different brain regions, which illustrate the different regional and developmental differences in NMDA receptor expression between WT and *Mecp2*-null mice. P values: *p<0.05; **p<0.01; ***p<0.001; ****p<0.0001; #p=0.055; ^p=0.075.

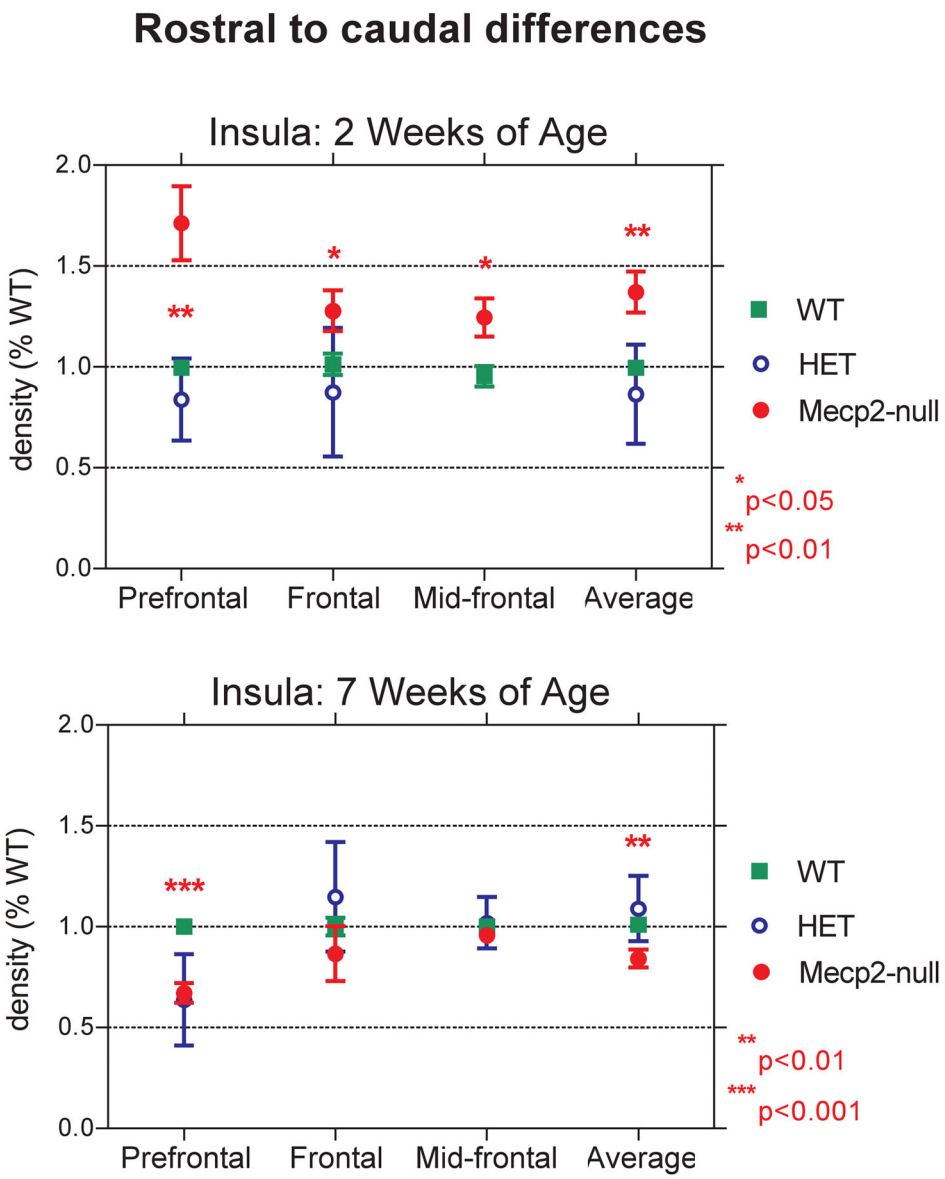

Figure 6.

Line graphs comparing the density of NMDA receptors between WT and *Mecp2*-null mice at 2 (A.) and 7 (B.) weeks of age at different rostrocaudal levels of the insula (percent WT; mean ± s.e.m.). P values: *p<0.05; **p<0.01; ***p<0.001.

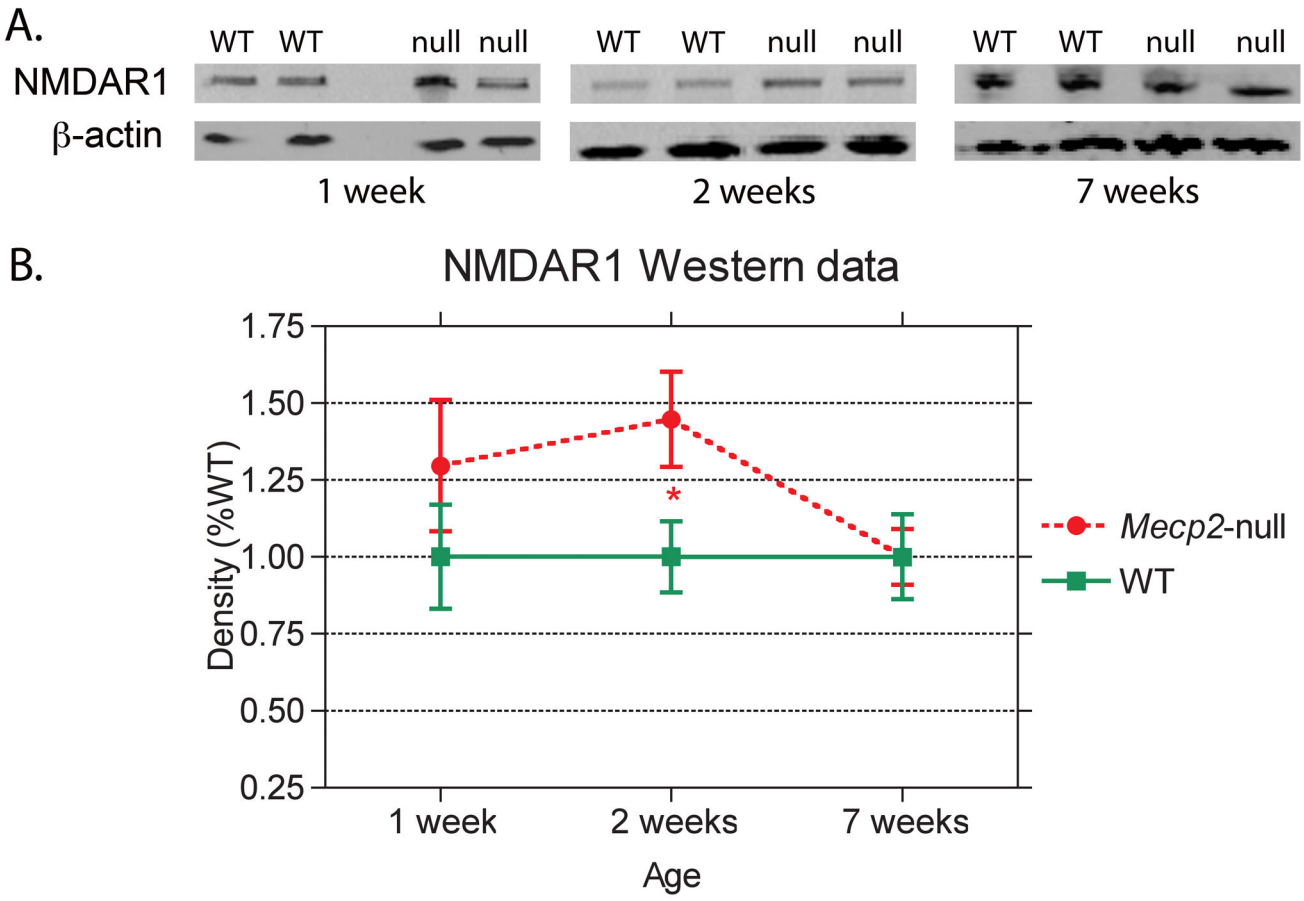

Figure 7.

Western blots of the NMDAR1 subunit of the NMDA receptor and β-actin from WT and Mecp2-null (null) mice at 1, 2 and 7 weeks of age are shown in A. Mean densities of NMDA1 protein (percent WT; mean ± s.e.m.) show a significant increase in NMDAR1 expression in Mecp2-null mice at 2 weeks of age but no genotype differences at 1 or 7 weeks of age (B.). P value: *p<0.05.

Table 1

Density of NMDA receptors in different brain regions

The mean density of [^{3}H] CGP binding to NMDA receptors ± s.e.m. (percent WT) in WT, HET and *Mecp2*-null mice at 2 and 7 weeks of age, and the p values for ANOVA for the three genotypes and for t-tests comparing WT versus *Mecp2*-null mice. For regions spanning different rostral to caudal levels through the brain (all except retrosplenial and visual cortex that were only measured at the level of the ventral hippocampus), values represent the average for all the different levels.

Region	WT	HET	*Mecp2*-null	ANOVA	t-test
2 weeks of age					
Frontal Motor Cortex	1.006±0.043	0.940±0.195	1.250±0.104	p=0.069	p=0.025*
Insula	0.995±0.027	0.864±0.246	1.371±0.102	p=0.003**	p=0.008**
Striatum	1.027±0.033	1.027±0.125	1.290±0.040	p=0.009**	p=0.001**
Somatosensory Cortex	1.007±0.036	0.933±0.117	1.126±0.075	p=0.182	p=0.132
Retrosplenial Cortex	1.000±0.044	1.003±0.178	1.346±0.163	p=0.051	p=0.019*
Visual Cortex	1.000±0.065	0.877±0.166	1.212±0.069	p=0.075	p=0.055
Thalamus	1.013±0.020	0.928±0.136	1.18±0.064	p=0.081	p=0.029*
Hippocampus	1.005±0.035	0.951±0.053	1.085±0.056	p=0.221	p=0.228
7 weeks of age					
Frontal Motor Cortex	0.994±0.037	1.020±0.223	0.676±0.024	p=0.038*	p<0.0001***
Insula	0.999±0.037	1.051±0.305	0.742±0.088	p=0.138	p=0.008**
Striatum	0.996±0.019	1.049±0.167	0.829±0.118	p=0.234	p=0.075
Somatosensory Cortex	1.000±0.026	1.030±0.169	0.755±0.023	p=0.032*	p<0.0001***
Retrosplenial Cortex	1.000±0.061	1.114±0.199	0.981±0.071	p=0.667	p=0.844
Visual Cortex	1.000±0.041	1.016±0.171	0.819±0.050	p=0.199	p=0.019*
Thalamus	1.008±0.045	1.124±0.161	1.257±0.053	p=0.038*	p=0.005**
Hippocampus	0.995±0.040	1.067±0.145	1.041±0.108	p=0.818	p=0.640

Table 2

Density of NMDA receptors in different level of the hippocampus at 2 weeks of age

The mean density of [^{3}H] CGP binding to NMDA receptors ± s.e.m. (percent WT) in 2 week-old WT (n=9–14) and *Mecp2*-null mice (n=4–8) and the p values for t-tests comparing WT versus *Mecp2*-null mice.

Level/Region	**WT**	***Mecp2*-null**	**t-test**
Dorsal Hippocampus			
CA1	1.040±0.064	1.062±0.146	0.873
CA3	1.053±0.060	1.092±0.114	0.744
CA3-Stratum Oriens	1.038±0.058	1.456±0.201	0.026*
CA3-Pyramidal cell layer	1.024±0.051	1.004±0.159	0.882
CA3-Stratum Radiatum	1.000±0.067	1.305±0.256	0.165
Dentate Gyrus	1.026±0.066	1.015±0.124	0.934
Hilus	0.993±0.088	0.932±0.136	0.702
Ventral Hippocampus			
CA1	1.023±0.038	1.184±0.104	0.089
CA3	1.043±0.041	1.240±0.052	0.018*
CA3-Stratum Oriens	0.997±0.065	1.450±0.223	0.018*
CA3-Pyramidal cell layer	0.985±0.030	1.202±0.077	0.005**
CA3-Stratum Radiatum	1.007±0.049	1.323±0.228	0.074
Dentate Gyrus	1.010±0.034	1.273±0.116	0.015*
Upper Blade Dentate Gyrus	1.027±0.060	1.171±0.128	0.268
Dentate Granular Cell Layer	1.000±0.051	1.299±0.092	0.006**
Hilus	1.012±0.0693	1.166±0.147	0.292
Subiculum	1.025±0.053	1.391±0.147	0.015*

Table 3

Density of NMDA receptors in different level of the hippocampus at 7 weeks of age

The mean density of [^{3}H] CGP binding to NMDA receptors ± s.e.m. (percent WT) in 7 week-old WT (n=8–9) and *Mecp2*-null mice (n=3–4) and the p values for t-tests comparing WT versus *Mecp2*-null mice.

Region	WT	*Mecp2*-null	t-test
Dorsal Hippocampus			
CA1	1.000±0.053	0.994±0.118	0.957
CA3	1.000±0.054	1.068±0.116	0.550
CA3-Stratum Oriens	1.000±0.084	0.750±0.201	0.230
CA3-Pyramidal Cell Layer	0.996±0.056	1.021±0.099	0.817
CA3-Stratum Radiatum	1.000±0.099	1.594±0.387	0.056
Dentate Gyrus	1.000±0.056	0.988±0.114	0.917
Hilus	1.000±0.048	0.867±0.109	0.218
Ventral hippocampus			
CA1	0.970±0.041	1.019±0.084	0.570
CA3	0.960±0.027	1.078±0.078	0.093
CA3-Stratum Oriens	1.002±0.028	1.266±0.164	0.037*
CA3-Pyramidal Cell Layer	0.952±0.048	0.939±0.095	0.890
CA3-Stratum Radiatum	0.989±0.027	1.293±0.128	0.006**
Dentate Gyrus	0.982±0.030	1.022±0.121	0.678
Upper Blade Dentate Gyrus	0.983±0.035	0.910±0.067	0.326
Dentate Granular Cell Layer	1.001±0.040	0.990±0.064	0.890
Hilus	0.971±0.036	0.919±0.121	0.588
Subiculum	0.933±0.072	0.793±0.125	0.354